Available online at www.sciencedirect.com
SCIENCE DIRECT
Polymer 46 (2005) 4431–4439
polymer
www.elsevier.com/locate/polymer

Hexadecyl-functionalized lamellar mesostructured silicates and aluminosilicates designed for polymer–clay nanocomposites. Part II: Dispersion in organic solvents and in polystyrene

Thuy T. Chastek[a], Andreas Stein[a], Christopher Macosko[b,*]

[a]Department of Chemistry, University of Minnesota, 207 Pleasant St. SE, Minneapolis, MN 55455, USA
[b]Department of Chemical Engineering and Materials Science, University of Minnesota, 421 Washington Ave. SE, Minneapolis, MN 55455, USA

Available online 24 March 2005

In honor of James E. Mark on the occasion of his 70th birthday

Abstract

Layered mesostructured silicates and aluminosilicates with covalently attached hexadecyl groups (denoted as C_{16}-LMS, C_{16}-LMAS, and a sample with layers whose thickness was increased by additional silicate, C_{16}-SiO_2-LMAS) were investigated as synthetic clays for dispersion and exfoliation in polymer melts. The dispersion of these clays in 13 organic solvents and their performance in polystyrene (PS) nanocomposites were examined. The three synthetic clays dispersed and formed gels in aromatic solvents and in a branched alkyl solvent (2,6,10,14-tetramethylpentadecane, TMPD) based on visual observations and rheology. The elastic moduli (G') of the toluene/clay dispersions for all three clays were similar when compared at equal inorganic content. The synthetic clays were blended with PS samples of various molecular weights. Melt rheology of the PS/clay nanocomposites showed a dramatic increase in elastic modulus compared with neat PS and formation of a G' plateau at low frequencies. The plateau occurred at higher G' values for C_{16}-LMAS than for C_{16}-SiO_2-LMAS or C_{16}-LMS, indicating that C_{16}-LMAS has higher strength and/or higher aspect ratio and can thus withstand the stresses of melt mixing. Increasing the molecular weight of PS increased G' of the PS/C_{16}-LMAS nanocomposites. By small angle X-ray (SAXS) and transmission electron microscopy C_{16}-LMAS showed better dispersion and a higher aspect ratio in the PS-nanocomposite than C_{16}-SiO_2-LMAS.

Keywords: Synthetic clays; Polystyrene; Polymer–clay nanocomposites

1. Introduction

Polymer/clay nanocomposites have received much attention lately due to their advantages for many industrial applications [1–5]. The most economical method for preparing nanocomposites is via direct blending of organically modified clays into polymer melts. However, this can be a challenge due to the immiscibility between commonly used non-polar polymers and the relatively polar, commercially available clays. A common approach to improve clay–polymer miscibility has been to add polymer compatibilizers to the blend [3,4,6–10]. Such compatibilizers must be designed for each polymer and they add to the cost of the nanocomposites. Typically, organically modified clays are prepared from natural clays through exchanging the native cations with cationic surfactants. This limits the amount and type of organic groups that can be inserted into the clay layers. Also, the relatively high temperatures employed in the melt blending process can lead to loss of the organo-modifiers [7,8,11,12].

To overcome both polymer–clay immiscibility and the limitations of organically modified natural clays we have investigated an approach to form polymer–clay nanocomposites without the need for a compatibilizer. Compatibility of clay sheets with non-polar polymers is instead provided by organic surface groups that are attached to inorganic layers in new synthetic clays. Three lamellar synthetic clay structures are examined here, mesostructured silicates with hexadecyl surface groups (C_{16}-LMS), similarly modified aluminosilicates (C_{16}-LMAS), and a sample with layers

* Corresponding author. Tel.: +1 612 6250092; fax: +1 612 6261686.
E-mail address: macosko@umn.edu (C. Macosko).

0032-3861/$ - see front matter © 2005 Elsevier Ltd. All rights reserved.
doi:10.1016/j.polymer.2005.02.062

whose thickness was increased by additional silicate groups (C_{16}-SiO_2-LMAS). We have described the syntheses and structures of these clays in a separate paper [13]. The sheets of C_{16}-LMS consist of single or double layers of tetrahedral silicate groups, each attached to a hexadecyl chain. C_{16}-LMAS is composed of pyrophyllite-like layers with an octahedral aluminum layer sandwiched between two tetrahedral silicate layers and hexadecyl surface groups. This structure is similar to montmorillonite, which is used as a starting clay for some commercial organoclays, but alkyl chains are covalently attached to the aluminosilicate layers and fill the spaces between layers. C_{16}-SiO_2-LMAS is structurally similar to C_{16}-LMAS; however, the presence of additional silicate groups in this material increases the inorganic layer thickness and introduces some structural disorder. The structures are shown schematically in Fig. 1. These synthetic functionalized clays can be expected to improve interactions between clays and non-polar polymers, miscibility, and degree of intercalation/exfoliation in non-polar polymers, since platelet–platelet interactions may be reduced by covalently bonding long alkyl chains to the clay layers and by decreasing the surface charge on the clay layers. Other thermodynamic interactions (polymer-surfactant and clay–clay interactions) are also modified by functionalization of the clays. Cloisite 20A is a commercial clay that has 1 nm thick aluminosilicate sheets, separated by cationic ditallow surfactant layers which are introduced in a separate ion-exchange step. In the present synthetic clays, problems associated with surfactant loss during melt blending are eliminated, because the surfactants are covalently attached to the inorganic layers during the clay syntheses in contrast to Cloisite 20A.

This paper presents investigations of the interaction between the synthetic clays and organic solvents, as well as the formation and performance of polystyrene (PS)/synthetic clay nanocomposites with PS samples of different molecular weights.

2. Experimental

2.1. Materials

PS samples with narrow polydispersity indices (PDI) and with two different molecular weights were generously donated by Dow Chemical: 18 kg/mol (PDI = 1.03), 50 kg/mol (PDI = 1.03). PS of 36 kg/mol (PDI = 1.15) was synthesized by atom transfer radical polymerization [14]. PS (PS-B-50K), which was purchased from Polyscience Inc, had a bimodal distribution of molecular weights [49 wt% of 1.3 kg/mol (PDI = 2.6) and 51 wt% of 91 kg/mol (PDI = 3.4)]. The syntheses and structure of the three synthetic clays C_{16}-LMS, C_{16}-LMAS, C_{16}-SiO_2-LMAS, were reported elsewhere [13]. We also used an organically modified montmorillonite, Cloisite 20A (Southern Clay).

2.2. Polymer–Clay nanocomposite preparation

The synthetic clays were blended with PS in a heated DACA twin-screw microcompounder with a typical sample size of 4 g [15]. A mixture of PS, synthetic clay, and the antioxidant Irganox (~0.01 wt%) was compounded under nitrogen at either 150 or 120 °C, 100 rpm for 15 min. These samples were molded directly into 25 mm diameter 1 mm thick disks on the rheometer plates.

2.3. Characterization

Small angle X-ray scattering (SAXS) was used to measure the extent of clay swelling (based on d_{001} values).

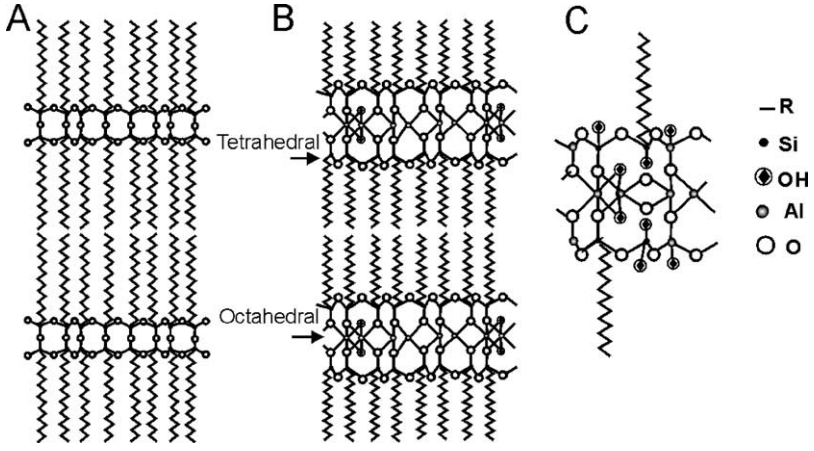

Fig. 1. Proposed schematic structures of the functionalized clays. Two possible structures for C_{16}-LMS include a single layer structure and a double layer structure which is shown in (A). The proposed structure of C_{16}-LMAS (B) contains both tetrahedral and octahedral Al present in the octahedral layer. In C_{16}-SiO_2-LMAS (C) additional silicate groups without alkyl chains are present and tetrahedral Al is likely to occupy some of the sites in tetrahedral layers. Terminal hydroxyl groups on tetrahedral Si are not explicitly shown in (A), or (B), but they are present. The alkyl chains in the diagram are schematic; no information about *trans-/cis-* configuration is implied.

A 0.58 m 2-D SAXS instrument with Cu Kα X-rays generated by a Rigaku RU-200BVH rotating anode was used. Solvent samples were sonicated for 3 h in an 8 mL vial, and prepared in 2 mm diameter capillary tubes, sealed with silicone glue. All samples were exposed for 15 min. Two-dimensional diffraction images were collected and corrected for detector response prior to analysis. Transmission electron microscopy (TEM) images were recorded digitally using a Jeol 1210 microscope operating at 120 keV. Thin sections (approximately 70 nm) of the PS nanocomposite materials were prepared by ultra-microtoming at room temperature using a Reichert Jung ultramicrotome with a diamond knife. From high magnification images the length and thickness of clay platelets were measured to calculate the aspect ratio, A_f.

2.4. Solvent tests and rheology

Clay miscibility and dispersion in several solvents were evaluated at clay contents ranging from 3–10 wt%. The mixtures were stirred in sealed 8 mL glass vials at room temperature (RT), and solvent clarity and viscosity were monitored visually. Rheological data were measured in duplicate at RT to study the interactions between the synthetic clays and solvents, using an ARES II rheometer (TA Instruments). A 50-mm parallel plate geometry was employed with a solvent trap to limit solvent evaporation. Melt state rheology data were obtained on an ARES rheometer at 150 °C. Samples were measured using 25 mm parallel plates with a gap of approximately 1 mm. Dynamic strain sweep and dynamic frequency sweep tests were performed on both solvent-clay dispersions and melt samples. A strain sweep was performed on each sample at a frequency of 1.0 rad/s and strains from 0.1 to 100%, to determine the linear viscoelastic (LVE) region. The critical strain was determined as the strain where G' had decreased to 80% of its maximum value. The frequency sweeps were performed from 100–0.01 rad/s at strains within the LVE region 10 min after the strain sweep.

3. Results and discussion

3.1. Interaction of the synthetic clays with selected solvents

The ability of the three synthetic clays (C_{16}-LMS, C_{16}-LMAS, and C_{16}-SiO_2-LMAS) to increase the viscosity of a series of solvents was investigated. This rapid screening test provides an initial indication of interactions between the clays and specific polymers with solubility parameters similar to those of the solvents.

Increases in the viscosity of synthetic clay-solvent mixtures were monitored visually. Even low concentrations of high aspect ratio, plate-like clay particles can lead to flocculation, caused by edge-to-face and edge-to-edge association ('house-of-cards' structures) and result in the formation of a continuous network or gel structure [16–19]. In this investigation, solvents were chosen based on their solubility parameters. Gel formation was observed after 10 days in solvent dispersions containing 5–10 wt% of clay. All synthetic clays were easily dispersed and formed gels with high thickening ability in aromatic solvents (Table 1). A strong gel formed in benzene, toluene, xylene, trimethylbenzene (TMB), and styrene for all three synthetic clays. The synthetic clays showed moderate affinity towards diethyl phthalate and 2,6,10,14-tetramethylpentadecane (TMPD), forming weaker gels with less thickening ability. The gel strength of C_{16}-LMAS and C_{16}-SiO_2-LMAS dispersions was observed to be higher than that of C_{16}-LMS at 3–10 wt% in aromatic solvents. The clays formed a weak gel in piperidine. The synthetic clays did not show affinity toward chloroform, dichloromethane, carbontetrachloride, THF, hexane, or cyclohexane (Table 1).

Table 1
Effect of solvent type on gelation

Solvent or polymer	Solubility parameter ($MPa^{1/2}$)[a]	Observations[b]
Polypropylene	16.6[c]	–
Polystyrene	17.9[c]	–
Hexane	14.9	Immiscible
2,6,10,14-TMPD	15.0[c]	Weak gel
Cyclohexane	16.8	Immiscible
Carbontetrachloride	17.6	Immiscible
Piperidine	17.8	Weak gel
Xylene	18.0	Gel
TMB	18.0	Gel
Toluene	18.2	Gel
Benzene	18.8	Gel
Styrene	19.0	Gel
Chloroform	19.0	Immiscible
Dichloromethane	19.8	Immiscible
Diethylphthalate	20.5	Weak gel

[a] [26].
[b] Same results for 5–10 wt% of C_{16}-LMS, C_{16}-LMAS, or C_{16}-SiO_2-LMAS.
[c] Calculated based on the method by Hoftyzer and Van Krevelen [27].

Small angle X-ray scattering (SAXS) of clay-solvent mixtures was used to measure the extent of clay swelling. No changes in the d_{001} values were observed, indicating that non-exfoliated material was still present and that it is not intercalated (Fig. 2). Since all samples had the same exposure time and experimental conditions, significant decreases in intensity of d_{001} peaks observed for 10 wt% C_{16}-LMAS or C_{16}-SiO_2-LMAS dispersions in toluene were interpreted as partial exfoliation of the clay layers during gel formation. This interpretation was strengthened by the much smaller decrease in intensity observed for a 10 wt% C_{16}-SiO_2-LMAS dispersion in hexane, an immiscible solvent for this clay. Nonetheless, the gel strength was observed to increase with increasing synthetic clay concentration in toluene. For clay/hexane dispersions, the gel strength followed the opposite trend. Thus, gel formation seemed

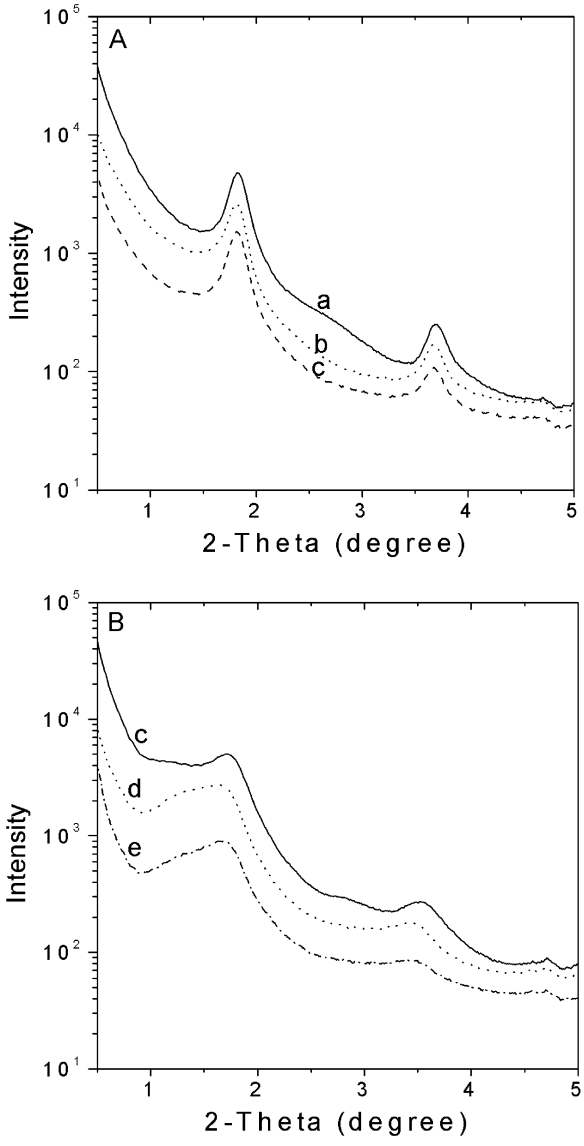

Fig. 2. SAXS analysis: (A) C_{16}-LMAS (a) as synthesized, (b) dispersed in hexane (10 wt% clay), and (c) dispersed in toluene (10 wt% clay); (B) C_{16}-SiO_2-LMAS (c) as synthesized, (d) dispersed in hexane (10 wt%), and (e) dispersed in toluene (10 wt% clay).

to have resulted from the percolation of a mixture of exfoliated and stacked clay platelets.

Rheology can provide more quantitative information about aggregation states of the clay particles and the extent of structural networking among individual silicate platelets [16–19]. Rheological measurements were carried out at RT for C_{16}-LMS, C_{16}-LMAS, C_{16}-SiO_2-LMAS at 3–10 wt% in toluene. All dispersions were aged for 10 days. Fig. 3(A) shows the elastic modulus, G' vs. strain amplitude at 1 rad/s for all three synthetic clays at 10 wt% in toluene. The strain limit of linear viscoelasticity is identified here as the strain where G' is 80% of its linear value (Table 2). All the critical strains are small, which is typical for flocculated suspensions. C_{16}-LMS has the highest critical strain. This higher critical strain, like its low G' values, may indicate that it is

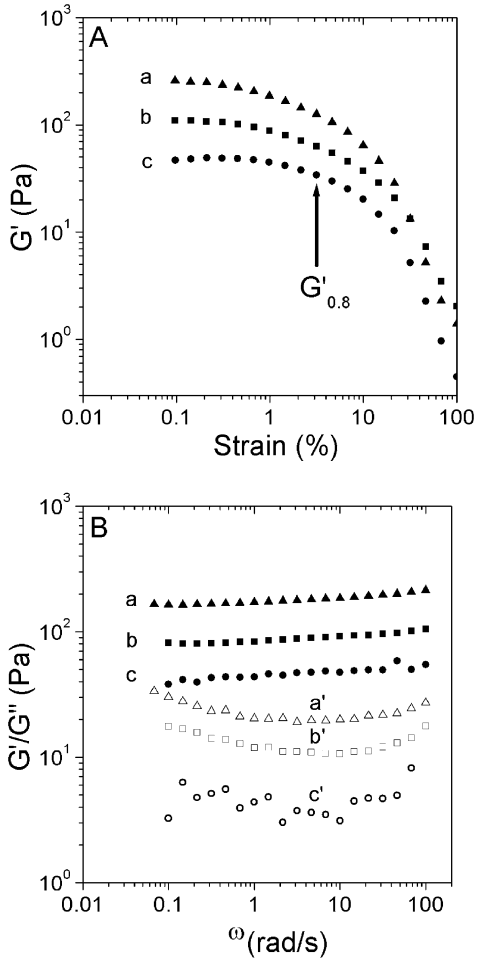

Fig. 3. Elastic moduli for clay dispersions at 10 wt% clay loadings in toluene at RT. (A) G' vs. strain: (a) C_{16}-SiO_2-LMAS, (b) C_{16}-LMAS, (c) C_{16}-LMS. (B) G' (a, b, c) and G'' (a', b', c').

the most flexible clay. C_{16}-LMS also has the highest organic content, which may result in longer range interactions between platelets and thus higher critical strain. G' is independent of frequency and higher than the loss modulus G'' for synthetic clays at 10 wt% loadings (Fig. 3(B)). This response indicates the presence of a weak elastic network. C_{16}-LMAS exhibits higher G' than C_{16}-SiO_2-LMAS, while G' for C_{16}-LMS is the lowest. The G' values at 1 rad/s in Fig. 3(B) are somewhat lower than the strain sweep values (Fig. 3(A) and Table 2). This is due to the fact that 10 min is not sufficient for the network structure to fully recover from the break down at 100% strain.

Changing the concentration from 3 to 10 wt% in toluene increased the elastic response and G' remained independent of frequency (Fig. 4(A)). This agrees with literature observations that increasing the concentration of a commercial organoclay increased the gel strength in organic solvents [16,18]. The increase from 3 to 5 wt% was much greater than from 5 to 10 wt%, similar to behavior reported for Cloisite 20A and fumed silica suspensions at this solid

Table 2
Plateau moduli and critical strain of toluene dispersions

Sample	Clay concentration (wt%)	Inorganic content of clay (%)	$G'_{plateau}$ (Pa)	Strain at $G'_{0.8}$ (%)
C_{16}-LMAS	3	0.9	4.0	1.8
	5	1.5	21.1	0.83
	10	3.0	110	0.99
	23	6.3	258	0.67
	10[a]	3.0	34.8	0.99
C_{16}-SiO_2-LMAS	3	1.1	6.1	0.31
	5	1.8	29.4	0.57
	10	3.6	251	0.67
	20	6.3	252	1.21
	10[a]	3.6	30.7	1.23
C_{16}-LMS	3	0.7	3.3	1.2
	5	1.2	19.3	1.23
	10	2.3	48.1	3.17
	28	6.3	240	0.99
	10[a]	2.3	5.8	2.67
Cloisite 20A	1.5	1.0	3.6	8.4
	2	1.3	9.0	5.7
	3	1.9	56.3	4.7
	5	3.2	590	2.3

[a] TMPD.

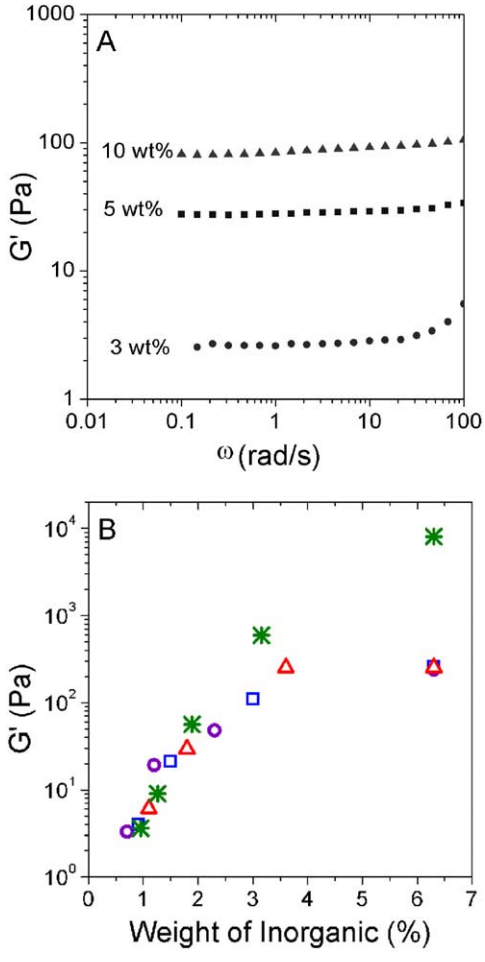

Fig. 4. (A) Elastic moduli for C_{16}-LMAS dispersions at 3–10 wt% in toluene. (B) Storage modulus G' as a function of clay loading in toluene for (△) C_{16}-SiO_2-LMAS, (□) C_{16}-LMAS, and (○) C_{16}-LMS and (*) Cloisite 20A.

loading [17,20,21]. Table 2 gives the plateau values of G' at 1 rad/s at the different clay concentrations.

It is useful to compare the synthetic clays at the same wt% inorganic since each has different mass fraction of covalently bonded organic groups. C_{16}-LMS also has the highest organic content, 77% compared to 70% for C_{16}-LMAS and 64% for C_{16}-SiO_2-LMAS. The stiff inorganic sheets are expected to dominate the rheological response. The wt% inorganic content is given in Table 2. When G' plateau values are plotted vs. wt% inorganic, all three synthetic clays and even cloisite 20A fall on about the same curve. This indicates that they are dispersed similarly in toluene. The onset of network formation appears to occur at about 0.5 wt% inorganic or about 0.2 vol% assuming a density of 2 g/cm^3 for the inorganic sheets. For this volume fraction, an aspect ratio, A_f, of about 190 would theoretically lead to percolation of random disks [22]. At high concentration the G' values become less dependent on concentration and all appear to converge to about 250 Pa at 6.3 wt% inorganic. This result agrees with reports by Zhong and Wang [17], who observed that G' becomes nearly independent of concentration above 4 wt% for Cloisite 20A in xylene. They attributed this to the gel 'freezing' the structure, preventing more exfoliation.

Fig. 5 shows the dynamic response of all three synthetic clay dispersions in TMPD at 10 wt% clay loading. All three synthetic clays show the presence of a weak elastic network. C_{16}-LMAS and C_{16}-SiO_2-LMAS have higher G' than C_{16}-LMS. In the branched alkyl solvent TMPD, G' was significantly lower than in toluene, consistent with the observation that the gel in TMPD was weaker (Fig. 5, Table 2). The solvent study indicated that the synthetic clays formed stronger gels with aromatic solvents than with linear, branched, or cyclic alkyl solvents.

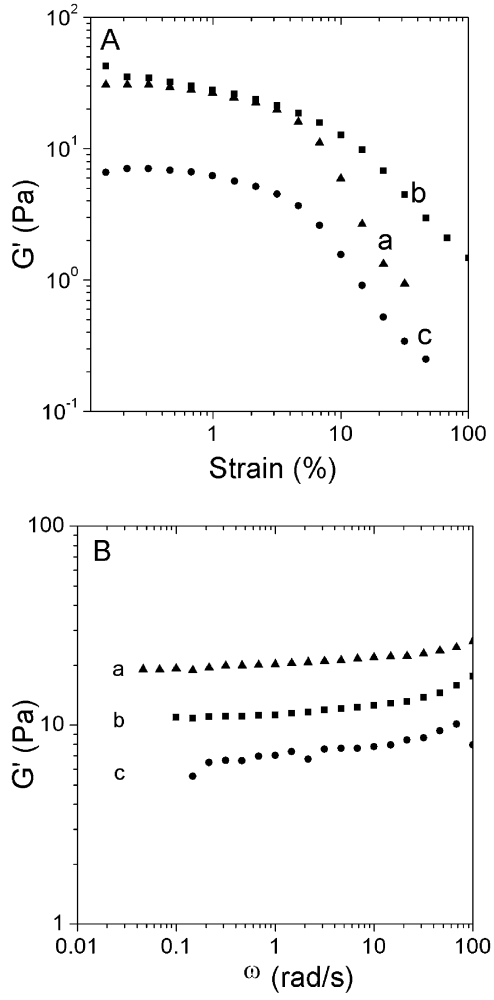

Fig. 5. Dynamic response (A) G' vs. strain and (B) G' vs. ω at 10 wt% clay loadings in TMPD: (a) C_{16}-SiO_2-LMAS, (b) C_{16}-LMAS, (c) C_{16}-LMS.

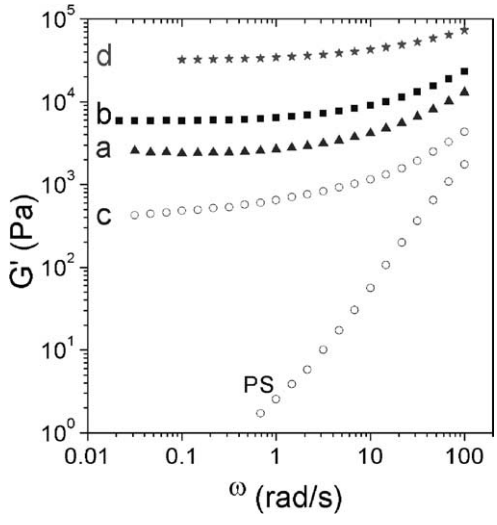

Fig. 6. Elastic moduli of PS/clay nanocomposites using PS-B-50K with (a) C_{16}-SiO_2-LMAS, (b) C_{16}-LMAS, (c) C_{16}-LMS, and (d) Cloisite 20A from melt rheology data obtained at $T=150$ °C, and 6.3 wt% inorganic material.

3.2. PS/Synthetic clay nanocomposites

3.2.1. Rheology

Nanocomposites of PS with clay loadings of 6.3 wt% inorganic content were prepared by melt blending. Since the fraction of inorganic material in each of the synthetic clays studied here was different, the value of 6.3 wt% inorganic content was chosen to allow direct comparison with the commercial clay Cloisite 20A, which has been widely studied in polymer nanocomposites. Melt rheology data showed a change from typical viscoelastic behavior for the neat PS to solid-like for the nanocomposites containing the synthetic clays (Fig. 6). Except for C_{16}-LMS, the plateau G' values are significantly higher than the values at 6.3 wt% inorganic in toluene. This is likely due to bridging between particles by the long PS chains and the high stresses experienced during melt mixing [23,24]. Octahedral aluminum in the sheets of C_{16}-LMAS and C_{16}-SiO_2-LMAS is believed to increase the stiffness and mechanical strength of the clay layers permitting these synthetic clays to retain higher aspect ratios after melt processing compared to C_{16}-LMS [13]. Even though the inorganic sheets are thickest in C_{16}-SiO_2-LMAS, the presence of layer defects [13] may have reduced the mechanical strength and aspect ratios of these platelets. Cloisite 20A, which has 1 nm thick aluminosilicate sheets, separated by cationic ditallow surfactant layers, gives the highest modulus in a PS matrix. This may be attributed to better dispersion and possibly higher layer stiffness due to higher crystallinity compared to the three synthetic clays.

3.2.2. TEM and SAXS

Fig. 7 shows TEM images of PS-B-50K nanocomposites with C_{16}-LMAS, C_{16}-SiO_2-LMAS, and Cloisite 20A. Exfoliated clay, as well as platelet stacks and flocculated clays are visible. The particle sizes of C_{16}-LMAS and C_{16}-SiO_2-LMAS ranged from 0.9 to 1.3 μm and 0.7 to 0.9 μm, respectively (edge-to-edge) [13]. The aspect ratio was measured by the ratio of the length to the thickness of platelets in at least five high magnification TEM images. All particles were included. The aspect ratios of clay particles in PS/C_{16}-LMAS range from 6 to 57 (average: 20 for 67 particles) while in PS-B-50K/C_{16}-SiO_2-LMAS they range from 6 to 20 (average: 12 for 33 particles) (Fig. 8). The high degree of dispersion and high aspect ratio of PS-B-50K/C_{16}-LMAS in TEM analysis agrees with the melt rheology data. The amount of octahedral aluminum in the sheets of C_{16}-LMAS is higher than in C_{16}-SiO_2-LMAS, and believed to increase the stiffness and mechanical strength of the clay layers permitting C_{16}-LMAS clays to retain higher aspect ratios after melt processing. The greater degree of dispersion and high aspect ratio in PS-B-50K/C_{16}-LMAS leads to a higher modulus G'. However, the degree of exfoliation is not as great as for PS-B-50K/Cloisite 20A (average: 26 for 46 particles) (Fig. 8(C)). It is possible that Cloisite 20A has higher crystallinity and a larger fraction of

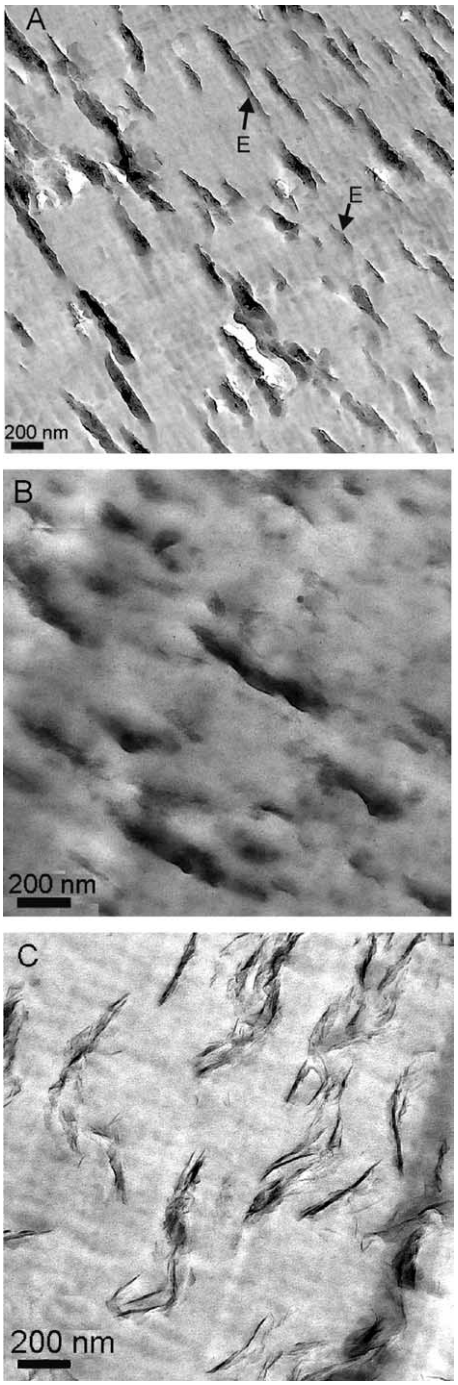

Fig. 7. TEM micrographs of (A) PS-B-50K/C_{16}-LMAS arrows labeled 'E' point at exfoliated clay sheets, (B) PS-B-50K/C_{16}-SiO_2-LMAS, and (C) PS-B-50K/Cloisite 20A blends. All blends contained 6.3 wt% inorganic material.

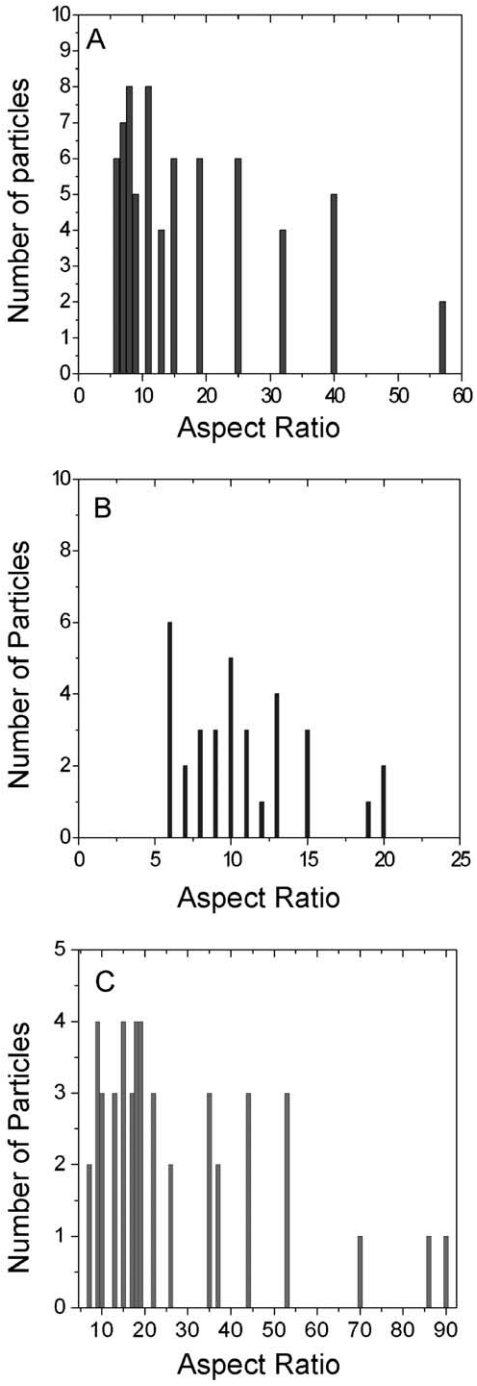

Fig. 8. Distributions of aspect ratios (particle length to thickness) for clay particles in blends, measured from TEM images for (A) PS-B-50K/C_{16}-LMAS, (B) PS-B-50K/C_{16}-SiO_2-LMAS, and (C) PS-B-50K/Cloisite 20A.

octahedral aluminum than the synthetic clays, helping it to retain the higher aspect ratio after the processing. Also, the presence of ditallow alkyl surfactant molecules (65% C_{18}, 30% C_{16}, 5% C_{14}), which are not covalently attached to the silicate layers, might weaken the interaction between layers. Thus, the polymer may replace the surfactant more easily, resulting in more exfoliation under shearing in the melt processing.

The first order reflection peaks in the SAXS traces of the blends did not shift, indication that no intercalation of the synthetic clays had occurred (Fig. 9). This is similar to the SAXS results in toluene and agrees with the observation of platelet stacks in the TEM micrographs [13]. The synthetic clays were found to have hydroxyl groups [13] that may have induced flocculation and reduced the degree of exfoliation. In addition,

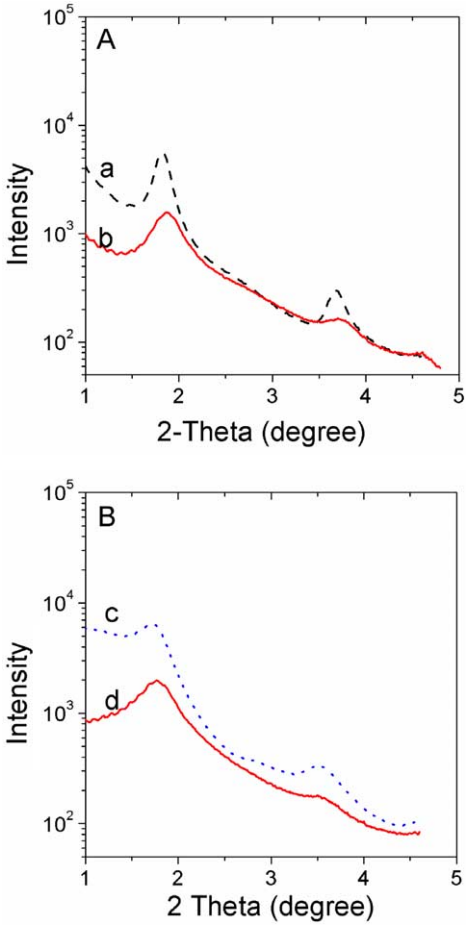

Fig. 9. SAXS analysis of (A) PS-B-50K/C_{16}-LMAS and (B) PS-B-50K/C_{16}-SiO_2-LMAS. (a), (c) clays as synthesized and (b), (d) PS/clay blends with 6.3% inorganic content.

the interaction between alkyl groups in the interlayer spacing may be so strong that platelets are prevented from fully exfoliating under shearing in melt processing. Furthermore, this strong interaction keeps multiple layers intact which in turn affects the appearance of the sheets in TEM micrographs of the blend compared to Cloisite 20A.

3.3. Effect of PS molecular weight

Lower molecular weight and higher blending temperatures cause a decrease in the viscosity of PS and thus lower the stresses on the clay particles. C_{16}-LMAS and C_{16}-SiO_2-LMAS were blended with narrow molecular weight PS samples of 18K, 36K, and 50K molecular weights at 150 °C. Melt rheology tests were carried out at 150 °C. The results are presented in Table 3 and compared to PS-B-50K. For C_{16}-SiO_2-LMAS, there was little effect of PS molecular weight on G'. Even the lowest stresses with PS 18K may be sufficient to break this synthetic clay. In C_{16}-LMAS blends, the elastic modulus G' increased significantly between PS 18K, 36K and 50K PS indicating that the higher mixing stress may have increased the degree of dispersion. By comparison, for composites of Cloisite 20A, the lowest molecular weight gave the highest G' value (Table 3) [25]. In this case Dogovskij et al. [25] have argued for increased ease of chain diffusion into the clay galleries.

4. Conclusions

The ability of the hexadecyl-functionalized synthetic clays to disperse and form gels in organic solvents was investigated. C_{16}-LMAS and C_{16}-SiO_2-LMAS formed stronger gels than C_{16}-LMS in selected aromatic solvents (toluene, xylene, benzene, styrene, and TMB) at 5–10 wt% by visual observation. The gels of all three clays were stronger in toluene than in a branched alkyl solvent (TMPD). This suggests that the synthetic clays are potentially more suited to be dispersed into PS, which is structurally more similar to aromatic solvents, than in polymers more akin to TMPD, such as polypropylene. Even though by SAXS the layer spacing did not change at 10 wt% in toluene, gel strength was observed to increase with the increasing clay concentration in toluene.

Dynamic rheology tests in toluene were used to confirm the gel formation, and to estimate the aspect ratio and flexibility of the synthetic clays. All three clays dispersed similarly, and form a network at roughly 0.2 vol% inorganic

Table 3
Plateau moduli G' of PS/synthetic clay blends with different PS molecular weights

	18k	36k	50k	50k bimodal	
Viscosity (Pa.s)	540	1400[a]	4300	3450[b]	
Sample	G'_{18}[b] (Pa)	G'_{36}[b] (Pa)	G'_{50}[b] (Pa)	$G'_{B\text{-}50}$[b,c] (Pa)	A_f
(Pa)					
C_{16}-LMAS	1.3×10^3	1.1×10^4	1.4×10^4	5.9×10^3	20
C_{16}-SiO_2-LMAS	1.2×10^3	1.2×10^3	3.1×10^3	2.6×10^3	12
C_{16}-LMS	–	–	–	4.3×10^2	–
Cloisite 20 A [25]	3.1×10^5	–	9.2×10^4	8.7×10^4	26

[a] Calculated.
[b] G' at 150 °C, 0.1 rad/s, and clay content 6.3% inorganic blended at 100 rpm, 15 min, 150 °C.
[c] Blended at 100 rpm, 15 min, 120 °C.

layers indicating that they have the same average aspect ratios. No change in modulus was observed for the three synthetic clays above 4% inorganic content in toluene. This implies that above a certain critical concentration, the gel prevents further exfoliation. The three synthetic clays had higher G' in toluene than in TMPD, in agreement with visual observations.

Composites obtained by melt blending PS with C_{16}-LMAS and C_{16}-SiO_2-LMAS had higher G' values than composites with C_{16}-LMS at the same 6.3% inorganic content, but not as high as with organically modified natural clay, Cloisite 20A. TEM analysis showed that clay sheets in PS/C_{16}-LMAS blends had a higher aspect ratio and clay particles were more exfoliated and better dispersed than in PS/C_{16}-SiO_2-LMAS blends, and both were significantly higher than C_{16}-LMS. The difference in response was attributed to breaking of C_{16}-LMS during melt mixing. C_{16}-LMS contained only silicate linkages in single or double layers. In C_{16}-LMAS, these were strengthened by incorporation of octahedral aluminum within silicate sheets. Rather than enhancing the mechanical stability, thickening of the layers in C_{16}-SiO_2-LMAS weakened the clay sheets slightly, because tetrahedral aluminum and hydroxyl defects were introduced.

Increasing the molecular weight of the PS matrix resulted in increased G' for C_{16}-LMAS but had no effect for C_{16}-SiO_2-LMAS. For C_{16}-LMAS blends, an increase in the molecular weight of PS resulted in stronger shear forces, which improved clay dispersion. For C_{16}-SiO_2-LMAS blends, two opposing effects may have resulted in the flatter response: the larger shear at higher molecular weight was offset by breakage of the mechanically weaker clay sheets into smaller particles.

Acknowledgements

This research was supported by grants from General Motors, the Industrial Partnership for Research in Interfacial and Materials Engineering (IPRIME) at the University of Minnesota, and by the MRSEC program of the NSF (Grant No. DMR-0212302). We thank Dr Steve Hahn of the Dow Chemical Company for donating PS 18K and PS 50K and Jianbin Zhang for synthesizing PS 36K, Dr Philippe Mongondry and Michail Dolgovskij for helpful discussions, and Kwanho Chang for TEM microtoming.

References

[1] Vu YT, Mark JE, Pham LH, Engelhardt M. J Appl Polym Sci 2001;82:1391–403.
[2] Alexandre M, Dubois P. Mat Sci Eng 2000;28:1–63.
[3] Kato M, Usuki A, Okada A. J Appl Polym Sci 1997;63:137–9.
[4] Karger-Kocsis J. Polypropylene: structure, blends, and composites. London: Chapman and Hall; 1995.
[5] Brune DA, Bicerano J. Polymer 2002;43:369–87.
[6] LeBaron PC, Wang Z, Pinnavaia TJ. Appl Clay Sci 1999;15:11–29.
[7] Cho JW, Paul DR. Polymer 2001;42:1083–94.
[8] Dennis HR, Hunter DL, Chang D, Kim S, White JL, Cho JW, et al. Polymer 2001;42:9513–22.
[9] Kato M, Usuki A, Okada A. J Appl Polym Sci 1997;66:1781–5.
[10] Wolf D, Fuchs A, Wagenknecht U, Kretzschmar B, Jehnichen D, Haussler L. Nanocomposites of polyolefins clay hybrids. Lyon-Villeurbanne: Eurofiller's 99; 1999. pp. 6–9.
[11] Fornes TD, Yoon PJ, Keskkula H, Paul DR. Polymer 2001;42:9929–40.
[12] Lincoln DM, Vaia RA, Wang ZG, Hsiao BS. Polymer 2001;42:1621–31.
[13] Chastek TT, Que EL, Shore JS, Lowy RJI, Macosko CW, Stein A. Polymer 2005;46 (this issue).
[14] Matyjaszewski K, Xia J. Chem Rev 2001;101:2921–90.
[15] Dolgovskij MK, Fasulo PD, Lortie F, Macosko CW, Ottaviani RA, Rodgers WR. Effect of mixer type on exfoliation of polypropylene nanocomposites. ANTEC 2003;2255–9.
[16] Luckham PF, Rossi S. Adv Colloid Inferface Sci 1999;82:43–92.
[17] Zhong Y, Wang Q. J Rheol 2003;47:483–95.
[18] Moraru VN. Appl Clay Sci 2001;19:11–26.
[19] Burgentzlé D, Duchet J, Gérard JF, Fillon B, Jupin A, Mueller C. Study of the dispersion of montmorillonite in organic solvents. Rheologie 2002. Morphologie et Structure, GFRSt-Etienne (France).
[20] Khan SA, Zoeller NJ. J Rheol 1993;37:1225–35.
[21] Kawaguchi M, Mizutani A, Matsushita Y, Kato T. Langmuir 1996;12:6179–83.
[22] Ren J, Silva S, Krishnamoorti R. Macromolecules 2000;33:3739–46.
[23] Krishnamoorti R, Giannelis EP. Macromolecules 1997;30:4097–102.
[24] Giannelis EP, Krishnamoorti R, Manias E. Adv Polym Sci 1999;138:107–45.
[25] Dolgovskij MK, Lortie F, Macosko CW. In: Annual technical conference—society of plastics engineers, 62, 2004. p. 1336–40.
[26] Brandrup J, Immergut EH, Grulke EA, Bloch DR, Abe A. Polymer handbook. 4th ed. New York: Wiley; 1999.
[27] Van Krevelen DW. Properties of polymer: their correlation with chemical structures; numerical estimation and prediction from additive group contributions. 3rd ed. Amsterdam: Elsevier Science; 1990.